TRANSIENT CHAOS IN DISSIPATIVELY PERTURBED, NEAR-INTEGRABLE HAMILTONIAN SYSTEMS

by

M. A. Lieberman and K. Y. Tsang

Memorandum No. UCB/ERL M85/26

12 April 1985

ELECTRONICS RESEARCH LABORATORY

College of Engineering
University of California, Berkeley
94720

Transient Chaos in Dissipatively Perturbed, Near-Integrable Hamiltonian Systems

M. A. Lieberman and Kwok Yeung Tsang

Department of Electrical Engineering and Computer Sciences
and the Electronics Research Laboratory
University of California, Berkeley, CA 94720

ABSTRACT

When near-integrable Hamiltonian systems are perturbed by dissipation, then the stable orbits become simple attracting sinks, the KAM tori are destroyed, and persistent chaotic motion disappears. We determine analytically the mean lifetime, the quasistatic distribution, and the fraction trapped into the various sinks for a dissipatively perturbed area-preserving twist map.

Two dimensional, near-integrable, measure-preserving maps are used to model conservative physical phenomena in such fields as celestial mechanics, cosmic ray physics, accelerator theory, and plasma heating and confinement.[1] Conservative systems of two, nonlinear, coupled oscillators are also used widely as physical models. This system motion also generates such maps as the phase space orbit repeatedly pierces a surface of section.

The phase plane structure in near-integrable measure-preserving maps is well known.[2] There is persistent regular motion on some perturbed KAM orbits and on KAM "island" orbits surrounding stable fixed points of the map. Regions of persistent chaotic motion are densely interwoven with these regular regions. The measures of the regular and the chaotic regions can vary widely, both within the phase plane and as a function of the system parameters.

This structure is not stable under dissipative perturbation. The stable fixed points become attracting centers (sinks), and all KAM curves are destroyed. Although transient chaotic motion generally exists, the phase point eventually enters an embedded island and is attracted to an island sink; the motion ultimately becomes periodic. The complete destruction of persistent chaos when a weak dissipation is added to a near-integrable Hamiltonian system is typical and probably generic behavior. It is clearly of interest to understand this degeneration from persistent to transient chaos.

In this letter, we present the first study of transient chaotic motion for a class of near-integrable Hamiltonian twist maps[2] that are perturbed by dissipation. We determine analytically such properties as the mean lifetime for chaotic motion, the quasistatic distribution for the transiently chaotic region, and the probability of trapping into the various embedded islands.

We note that above a critical dissipation strength, a new type of attractor ("strange" attractor) in the phase plane can appear, on which the motion is persistent and chaotic.[3-5] We have considered this case elsewhere.[6-7]

We illustrate the calculation procedure for transient chaos using as an example the dissipative Fermi map.[6-7] However, the procedure is directly applicable when dissipation is introduced into other twist maps such as the Chirikov-Taylor[8-9] and the separatrix maps.[2,8] The Fermi map describes a cosmic ray acceleration mechanism[10] in which charged particles are accelerated by collisions with moving magnetic field structures. In the model, a ball bounces in one-dimensional motion between a fixed and an oscillating wall. We adapt a simplified model[11] in which the moving wall oscillates sinusoidally, $x_w(t) = a \cos \omega t$, and elastically imparts momentum to the ball according to its velocity $\dot{x}_w$ without the wall changing its position in space. We introduce dissipation by assuming that the ball suffers a fractional loss δ in velocity upon collision with the fixed wall. The map is then

$$\bar{u} = (1-\delta)u_n - \sin\psi_n \quad , \tag{1a}$$

$$\bar{\psi} = \psi_n + 2\pi M/\bar{u} \quad , \tag{1b}$$

$$(\psi_{n+1}, u_{n+1}) = (\bar{\psi}, \bar{u}) \operatorname{sgn} \bar{u} \quad , \tag{1c}$$

where $u_n = v_n/(2\omega a)$ is the normalized ball velocity and $\psi_n = \omega t_n$ is the phase of the oscillating wall, and $M = l/(2\pi a)$ is the normalized distance between the two walls. The function $\operatorname{sgn} \bar{u} = \pm 1$ for $\bar{u} \gtrless 0$, and is introduced to maintain $u_{n+1} \geq 0$ for low velocities $u_n < (1-\delta)^{-1}$, as physically occurs in the exact model, while preserving the continuity of the map near $u = 0$. The Jacobian of the map is $1 - \delta$, and thus the map is area-preserving for $\delta = 0$.

The primary fixed points of the map are found by setting $u_{n+1} = u_n$ and $\psi_{n+1} = \psi_n (\text{mod} 2\pi)$ in (1). We obtain

$$(u_k, \psi_k) = (M/k, \sin^{-1}(-u_k \delta)), \tag{2}$$

where k is an integer. There are two fixed points for each k : $\psi_k \approx 0$ or $\psi_k \approx \pi$ for $u_k \delta \ll 1$. $\psi_k \approx \pi$ is stable for $u_k > u_s = (\pi M/2)^{1/2}$; $\psi_k \approx 0$ is always unstable. For $\delta = 0$, invariant (KAM) island orbits surround the stable fixed points.

We summarize the behavior of the motion, determined by numerical iteration, as the parameters M and δ are varied. For $\delta = 0$, there is no dissipation and the usual Hamiltonian chaos ensues, with intermingled areas of persistent chaotic and regular motion in the $(u - \psi)$ phase plane. Numerical iterations for $10 \lesssim M \lesssim 10^4$ show[11-14] that the phase plane divides into three characteristic regions: (1) For large velocities, $u > u_b \approx 2u_s$, invariant (KAM) curves span the plane in ψ and isolate the narrow layers of stochasticity near the separatrices surrounding the fixed points of the map; (2) there is an interconnected stochastic region for intermediate velocities, $u_b > u > u_s$, in which invariant islands near stable fixed points of the map are embedded in a stochastic sea; and (3) there is a predominantly stochastic region for small velocities, $u < u_s$, in which all primary fixed points are unstable. The globally stochastic motion within the connected regions (2) and (3) is isolated from region (1) by a KAM barrier at u_b, and has a constant equilibrium invariant distribution $f_0(u, \psi)$.[15]

For weak dissipation, $0 < \delta < \delta_c$, the numerical iterations show that the fixed points of the Hamiltonian map become attracting centers (sinks), the KAM curves no longer exist, and all persistent chaotic motion is destroyed. However, transient chaotic motion surrounds the sinks in regions (2) and (3). As an example, for $M = 30$ ($\delta_c \approx .02$) and $\delta = .003$, we find that an initial phase point chosen randomly in region (3) undergoes transient chaotic motion for a mean number of iterations $\bar{N} \approx 13{,}000$ before it enters an embedded island in region (2) and becomes trapped in an island sink. The decay rate $\bar{\alpha} = \bar{N}^{-1}$ is tabulated for various values of M and δ in Table 1.

In Fig. 1, we plot the cumulative phase-integrated distribution

$$\mathcal{F}(u) = 100 \int_0^N dn \int_0^{2\pi} d\psi\, f(u,\psi,n)$$

for $M = 30$, $\delta = .003$, after $N = 5 \times 10^4$ iterations, for 100 initial conditions at low velocities chosen randomly. We see evidence of attracting sinks near the primary resonances at $k = 3$ (a period 1 and a period 5 sink coexist) and at $k = 4$ (a period 1 and a period 3 sink coexist). Numerical studies for various values of N, M and $\delta \ll 1$ show that an exponentially decaying quasistatic distribution

$$f(u,\psi,n) = f_Q(u)\exp(-\bar{a}n) \tag{3}$$

for values of u outside of the "sticky" islands, is formed for $n \gtrsim u_b^2 \approx 2\pi M$.

The distribution f_Q can be found analytically by solving the appropriate Fokker-Planck equation for the map[16]

$$\frac{\partial f}{\partial n} = \frac{1}{2}\frac{\partial}{\partial u}\left(D\,\frac{\partial f}{\partial u}\right) - \frac{\partial(Bf)}{\partial u} \approx 0 \tag{4}$$

where, to first order in δ, D is the diffusion coefficient for the area-preserving ($\delta = 0$) map, and $B = -u\delta$ is the friction coefficient due to the dissipation.[15] For $u \lesssim u_s$, $D = 1/2$, the quasilinear value. However, the domain of interest includes the region $u_s \lesssim u \lesssim u_b$, in which the quasilinear diffusion coefficient is invalid. To obtain an estimate of D in this region, we locally expand (1) in u about a fixed point u_k, which yields

$$I_{n+1} = I_n(1-\delta) + K \sin \vartheta_n - u_k\delta\ , \tag{5a}$$

$$\vartheta_{n+1} = \vartheta_n + I_{n+1}\ , \tag{5b}$$

where

$$I_n = -K(u_n - u_k) \tag{6a}$$

$$\vartheta_n = \psi_n \ , \tag{6b}$$

and

$$K = 2\pi M / u_k^2 \tag{7}$$

is the stochasticity parameter. For $\delta = 0$, (5) is the Chirikov-Taylor or "standard" map,[17] which has a diffusion coefficient $\bar{D}$ that depends on K. For $K \gtrsim 4$, corresponding to $u \lesssim u_s$, $\bar{D} \approx K^2/2$, the quasilinear value. For $4 \gtrsim K > 1$, corresponding to $u_s \lesssim u < u_b$, one finds

$$\bar{D} \propto (K-1)^\gamma \ ,$$

with the estimate[8] $\gamma \approx 2.5$ for $4 \gtrsim K > 1$ obtained numerically, and the asymptotic result[18-19] near $K = 1$, $\gamma \approx 3.01$. However, over the entire $K > 1$ range, a reasonable fit to the numerical data for $\bar{D}$ is

$$\bar{D} \approx \frac{K^2}{2}\left(\frac{K-1}{K}\right)^2 \ , \tag{8}$$

with $\gamma = 2$. Transforming from I back to u, we have $D = \bar{D}/K^2$, and using (7) and (8), we obtain, for $u < u_b$,

$$D = \frac{1}{2}\left(1 - \frac{u^2}{u_b^2}\right)^2 \ . \tag{9}$$

Using (9) in (4) and the condition that the net flux is zero, we obtain

$$f_Q(u) = F \exp[-2\beta u^2/(u_b^2 - u^2)] \ , \tag{10a}$$

where

$$F = (2\pi u_b \beta)^{-1}[K_1(\beta) - K_0(\beta)]^{-1}\exp(-\beta) \ , \tag{10b}$$

$\beta = u_b^2\delta$, K_1 and K_0 are the modified Bessel functions, and

$$2\pi \int_0^{u_b} du f_Q(u) = 1 \ .$$

This distribution, scaled to the value of $\bar{f}$ at $u = 0$, is plotted as the dashed line in Fig. 1. The agreement with the numerical result outside the island regions is excellent. Equally good agreement is found for all other cases listed in Table 1.

We now determine the phase space area ΔA_k in the transiently chaotic region that is "eaten" by each primary island during one iteration. The standard map [(5) with $\delta = 0$] has a closed KAM barrier $I(\vartheta)$ with area $\bar{A}$ surrounding the central fixed point $(I, \vartheta) = (0, \pi)$. This barrier curve separates the outer chaotic region from the inner closed island orbits. For $\delta > 0$, $\bar{A}$ contracts by the factor 1 - δ. Thus $\Delta\bar{A} = \bar{A}\delta$. Transforming back to (u, ψ) variables using (6), we obtain

$$\Delta A_k(u_k) = \bar{A}\ \delta / K \ . \tag{11}$$

$\bar{A}$ is a function of $K = u_b^2/u_k^2$ alone that can be found analytically[19-20] or numerically[8]. A good approximation for $1 < K < 6$ is $\bar{A} \approx 2\pi^2 K^{-1.3}$. For the results in Table 1, we determine $\bar{A}$ numerically by setting $\delta = 0$ in the first term on the right hand side of (5a). The small correction in $\bar{A}$ due to the last term $-u_k\delta$ in (5a) was therefore included.

Using the (10) and (11), we obtain the decay rate for the transiently chaotic region

$$\bar{\alpha} = \sum_k \alpha_k \ , \tag{12a}$$

where

$$\alpha_k = f_Q(u_k)\Delta A_k \qquad (12b)$$

and the sum is over all stable primary fixed points u_k in the region $u_s < u < u_b$.

The first entry in Table 1 gives the exponential decay rate $\overline{\alpha}$ determined by numerical iteration of 100 random initial phase points at low velocities; the second entry gives the analytical result (12). The agreement is seen to be quite reasonable.

The fraction μ_k of initial phase points that stick to the various islands can also be found analytically using (12b). In Fig. 2, we plot the ratio $R_k = \mu_k$ (analytical)/μ_k (numerical) for all stable u_k for the cases in Table 1. For M = 30, k = 3, 4; for M = 100, k = 5-8; for M = 300, k = 9-16. We see that (12b) agrees well with the numerical results. Even better agreement is obtained using $\gamma = 3$ in (8), particularly for those islands that are close to the adiabatic barrier u_b. We expect a better estimate for $\overline{D}$ in (8) to yield even closer agreement to the numerical results for $\overline{\alpha}$ and μ_k.

Several additional features observed numerically remain to be brought within the framework of the theory presented here. In several cases in Table 1, a few of the hundred initial conditions were attracted to a primary resonance having period two. These resonances, $u_{n+2} = u_n$, $\psi_{n+2} = \psi_n$ (mod 2π), are located near $u_k \approx 2M/k$, k odd, and are stable within some parts of region (2). We believe the effect of these higher period sinks can be treated analytically by considering the square, cube, etc. of the map (1).

For the case M = 100, the stochasticity parameter for the k = 8 fixed point at $\delta = 0$ is $K \approx 4.02$. Thus this fixed point is linearly unstable, and a stable, bifurcated periodic orbit appears nearby.[2] However, a KAM barrier having area $\overline{A}$ still surrounds this period two orbit. The size of $\overline{A}$ depends delicately on δ. Thus we determined $\overline{A}$ by numerically iterating the map (5) with δ set to zero in the first term on the right hand side of (5a). In general, the areas of the stable period two, four, etc. islands are small.

Another numerical observation is that within each island surrounding a primary sink at u_k, there are a number of secondary sinks having periods greater than one. For example, Fig. 1 shows a period 5 secondary sink surrounding the primary sink at $u_3 = 10$, and a period 3 secondary surrounding the primary sink at $u_4 = 7.5$. We determined in (12) only the total fraction of initial orbits eaten by an island, and not the distribution among the primary and secondary sinks within the island. We believe the latter distribution might be determined by first transforming to obtain the separatrix mapping[2,8] associated with the primary resonance u_k and then by applying the theory presented here to the separatrix mapping. The procedure for effecting this renormalization transformation from primary to secondary resonances is described in reference 1, secs. 2.4 and 4.3.

The support of the Office of Naval Research contract N00014-84-K-0367 and the National Science Foundation grant ECS-8104561 is gratefully acknowledged.

References

[1]A. J. Lichtenberg and M. A. Lieberman, *Regular and Stochastic Motion*, Springer-Verlag, New York, (1982), Appendix A.

[2]Reference 1, Ch. 3.

[3] R. H. G. Helleman, in *Fundamental Problems in Statistical Mechanics*, Vol. 5, E. G. D. Cohen (ed.), North Holland, Amsterdam, (1980), p. 165.

[4]R. Shaw, Z. Naturforsch. **36A**, 80(1981).

[5]E. Ott, Rev. Mod. Phys. **53**, 655(1981).

[6]K. Y. Tsang and M. A. Lieberman, Physica **11D**, 147(1984).

[7]K. Y. Tsang and M. A. Lieberman, Phys. Lett. **103A**, 175(1984).

[8]B. V. Chirikov, Phys. Reports **52**, 263(1979).

[9]G. M. Zaslavskii, Phys. Lett. **69A**, 145(1978).

[10]E. Fermi, Phys. Rev. **75**, 1169(1949).

[11]M. A. Lieberman and A. J. Lichtenberg, Phys. Rev. **A5**, 1852(1972).

[12]G. M. Zaslavskii and B. V. Chirikov, Soviet Physics Doklady **9**, 989(1965).

[13]A. Brahic, Astr. and Astrophys. **12**, 98(1971).

[14]A. J. Lichtenberg, M. A. Lieberman and R. H. Cohen, Physica **1D**, 291(1980).

[15]Reference 1, pp. 436-442.

[16]Reference 1, sec. 5.4.

[17]Reference 1. sec. 4.1.

[18]A. B. Rechester, M. N. Rosenbluth and R. B. White, Phys. Rev. **A23**, 2664(1981).

[19]N. M. Murray, M. A. Lieberman and A. J. Lichtenberg, "Corrections to Quasilinear Diffusion in Area-Preserving Maps," Electronics Research Laboratory Report UCB/ERL M84/102, University of California, Berkeley; submitted to Phys.

Rev. A (1985).

[20] A. J. Lichtenberg, Nucl. Fusion **24**, 1277(1984).

CAPTIONS

Table 1. Numerically/analytically determined decay rates $\overline{\alpha}$ (in units of 10^{-5}), for various values of M and δ.

Fig. 1. Cumulative, phase-averaged distribution $\overline{f}$ versus u, for M = 30, δ = .003, $N = 5 \times 10^4$ iterations. The solid curve shows the numerical result; the dashed curve shows the quasistatic theory.

Fig. 2. The ratio R_k of the analytically-to-numerically determined fractions μ_k of initial phase points attracted to the various island sinks, for all the cases given in Table 1.

Table 1

M \ δ	.0003	.001	.003	.01
30	2.0/2.5	2.7/6.6	7.4/12.0	7.7/8.6
100	1.2/2.0	2.0/3.6	2.9/2.6	1.1/.29
300	1.1/1.1	1.1/.90	.40/.16	

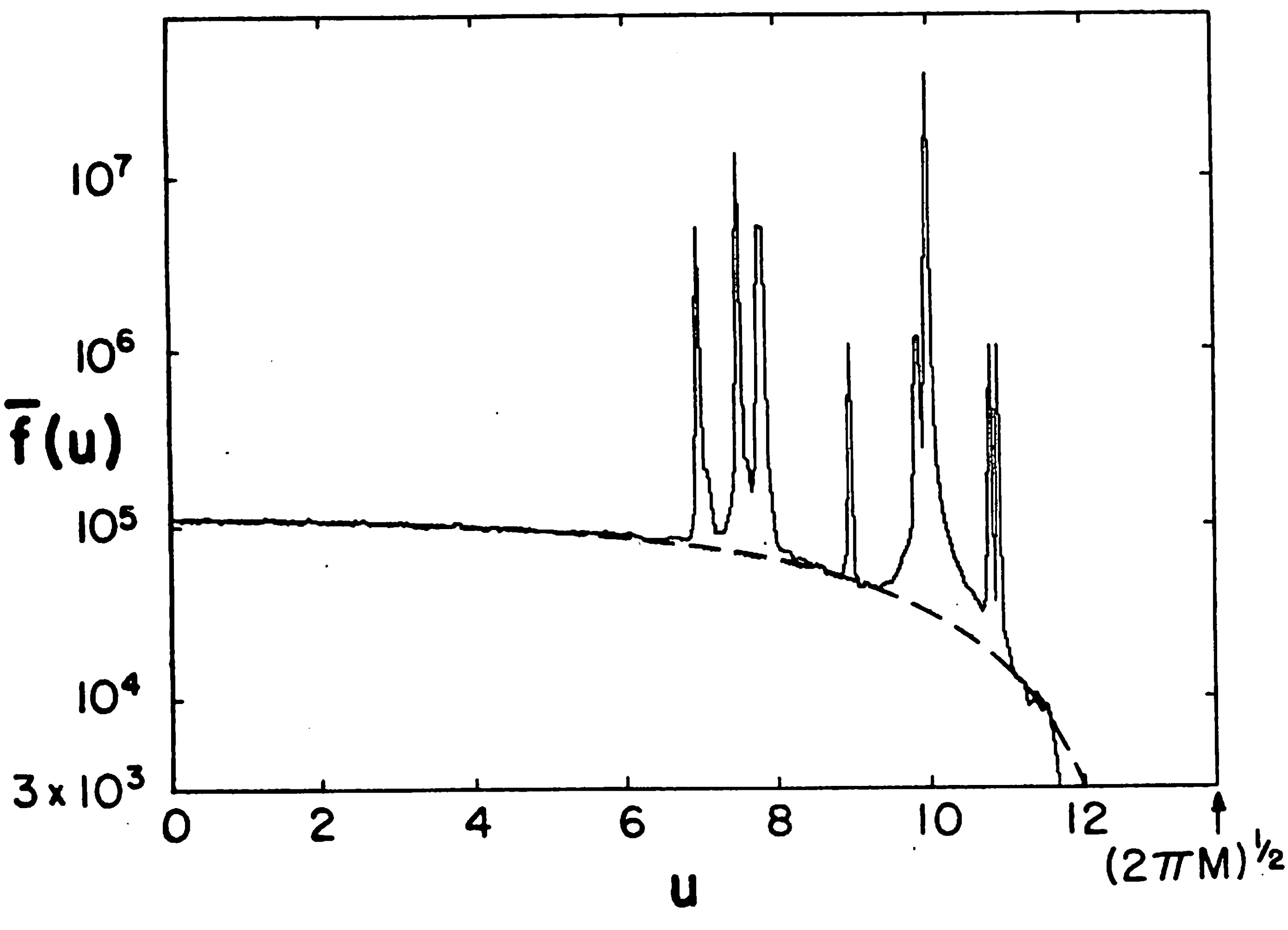

FIGURE 1

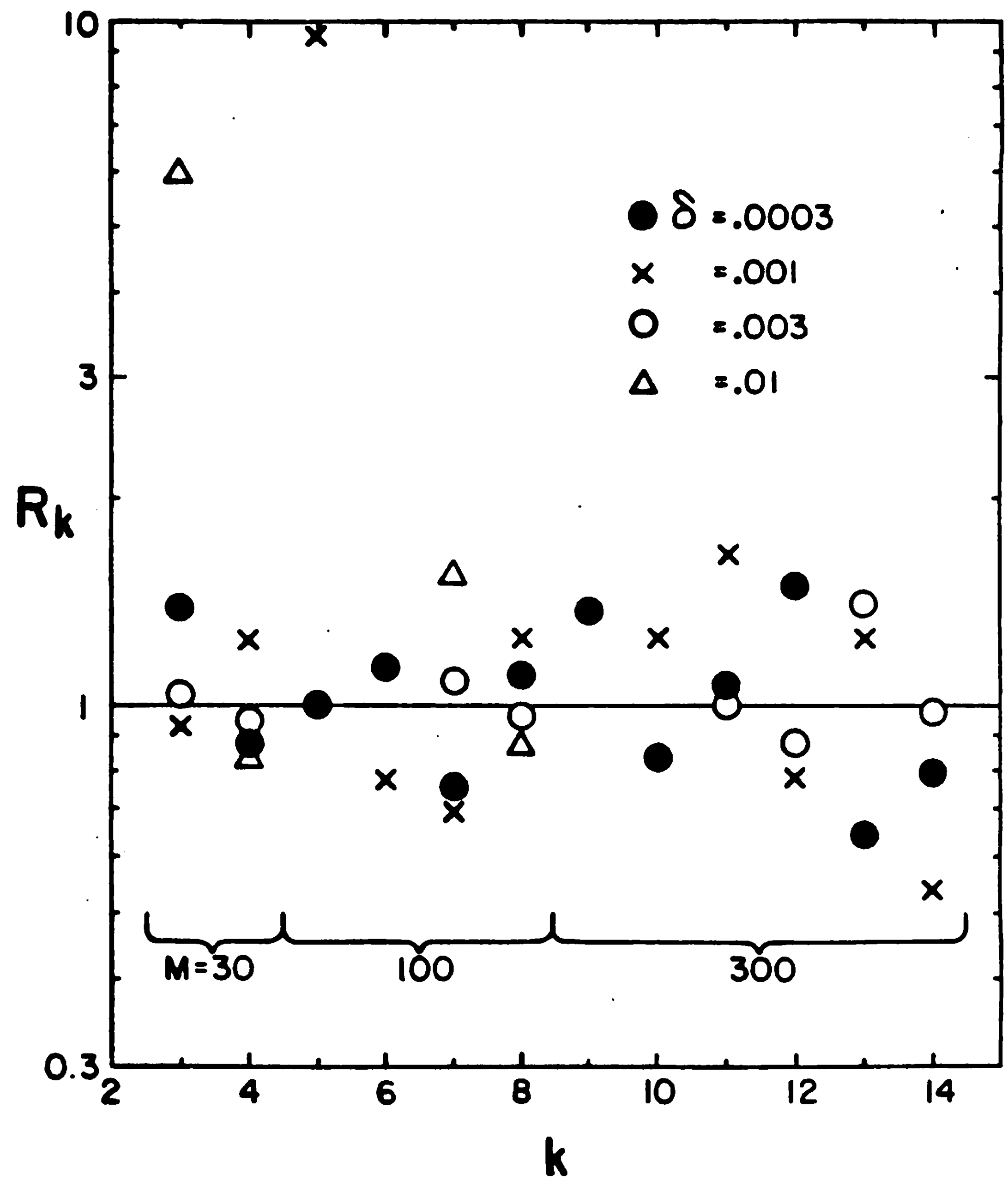

FIGURE 2